# Fluxes and excess temperatures of mantle plumes inferred from their interaction with migrating mid-ocean ridges

**Jean-Guy Schilling**

Graduate School of Oceanography, The University of Rhode Island, Kingston, Rhode Island 02881, USA

The behaviour of thermal plumes in the Earth's upper mantle is strongly affected by their interaction with nearby mid-ocean ridges. The magnitude of the buoyant topography and the length of the geochemical anomaly induced by plumes at migrating ridge axes provide a way to estimate their excess temperature and discharge rate, and thereby constrain their depth of origin.

IT is now generally accepted that the Earth's mantle is convecting. The different scales and styles of convection, however, remain uncertain[1-3]. Broadly speaking, the convective structure of the mantle is composed of at least two thermal boundary layers where horizontal flow dominates: one at the core–mantle boundary, the other just beneath the lithospheric plates near the Earth's surface. Some assume that a third thermal boundary layer is present at the 670-km discontinuity, but this is controversial[4]. Downward movements seem to be dominated by arcuate sheets associated with the subduction of the lithospheric plates observed near trenches and island arcs. In contrast, hot mantle upwellings appear columnar and plume-like. Mid-ocean ridges, which migrate relative to the plumes as a result of the global integration of forces acting on plates[5], seem to be passive features tapping merely upper-mantle material in response to plate divergence. On the other hand, rising mantle plumes, such as beneath Hawaii or Iceland, more directly reflect the convective state of the deeper mantle. This rough picture is based on surface observables such as plate tectonics, heat flow, the geoid and topographic swells and lineaments[6-8], and three-dimensional constraints from seismic tomography[9] and from numerical and laboratory studies of fluid dynamics[3].

Here I focus on the interaction and the dispersal of plumes in the upper mantle, using the spatial distribution of isotope and trace element ratios in basalts from mid-ocean ridges and ocean islands as tracers of mantle dynamics[10,11], much as dyes are used to follow flow patterns and mixing conditions in laboratory studies of fluid dynamics. This is possible because mantle plumes are isotopically distinct from the asthenosphere which normally feeds the mid-ocean ridges[11,12]. This tracer approach, combined with topographic anomalies, provides a means of constraining the volumetric flux of plumes and their excess temperatures relative to the asthenosphere.

On this basis, I evaluate the effect of migrating ridges on the dispersal of mantle plumes. Plumes now as much as 1,000 km from a ridge seem to continue to discharge practically entirely into migrating ridges, which act as sinks. Of the 13 plumes investigated (Fig. 1), the discharge rates range from 0.4 to 3 $km^3\ yr^{-1}$. Remarkably, the excess temperatures of these plumes fall in the narrow range of 160–280 K, and their variations are apparently independent of their volumetric flux. For

comparison, the flux of the purely intraplate Hawaiian plume is 9–12 $km^3\ yr^{-1}$, and its excess temperature is 225–300 K (refs 7,13). The excess temperatures of these plumes are also independent of their distance to the migrating ridge involved and of their compositional diversity as reflected by their isotope ratios of helium, lead, neodymium and strontium. These surprising results suggest that a quasi-steady thermal state is rapidly established between the thermal plume, the asthenosphere and the accreting and aging lithosphere from the time these plumes were ridge-centred. They also indicate a common, heat-regulated, source in the mantle, which I suggest is likely to be the D″ thermal boundary layer at the core–mantle interface.

## Plume dispersal models

Several plume dispersal models are currently being debated. For instance, White and McKenzie[14] consider that plumes disperse horizontally beneath the rigid lithosphere in an essentially radial fashion over distances of 1,000–2,000 km. By contrast, Sleep[13] considers that drag from the plate skews the dispersal of intraplate plumes injected into the low-viscosity zone beneath the lithosphere.

The blob-cluster model suggests that the breakup and dispersal of mantle plumes is directly proportional to the convective rate of the upper mantle, as measured by the spreading rate of mid-ocean ridges[15]. It implies a direct link between mantle convection and relative plate motions, and an inverse relationship between spreading rate and variance in isotopic composition in MORBs (mid-ocean-ridge basalts).

Plumes tilted markedly in the upper mantle by plate drags, or by deeper return flows associated with the subduction of plates, may enhance entrainment of the surrounding mantle and detachments of blobs once a critical tilt angle is reached[16–18].

I have pursued the mantle-plume source/migrating-ridge sink (MPS/MRS) model, which suggests that the migrating ridge is fed and dynamically affected by a preferential plume flow along a thermally induced channel at the base of the lithosphere. The inverted channel is progressively carved by the hot plume from the time it was ridge-centred[10,11,19] (Fig. 2). When ridge-centred, the preferential plume flow takes place along the ridge axis, roughly symmetrically about the plume[10,20,21]. Mixing of the rising plume with the asthenosphere takes place by entrainment and in the melting zone, which is initiated at greater depth than along normal ridge segments because the plume is hotter. A larger mean degree of melting and a thicker crust result. A key feature is that if the model[10] is to generate the excess topography and the geochemical gradients observed, the plume flux must exceed the production rate of new lithosphere integrated along the ridge across the plume diameter (on-axis case, Fig. 2*a*), or over the width of the lateral plume channel at its intersection with the migrating ridge axis (off-axis case, Fig. 2*b*).

It is now well documented that mid-ocean ridges migrating away from hot mantle plumes are geochemically and dynamically affected by plumes discharging over long times ($t$) and ridge migration distances ($x$). The flow connection between plumes and migrating ridges has been established from the following surface observables: tracks of constructional volcanism[19], the geochemical anomaly length, $W$, along the ridge and the associated excess ridge elevation[10], $\Delta E$ (Fig. 2), and the identification of plumes from mixing vectors in multiple-isotope-space representations of basalt compositions[12,22].

The empirical relationships $W = 1{,}010 - 24.5x^{1/2}$ and $\Delta E = 2.42 \times 10^{-3} W$ (with $W$ and $\Delta E$ in km), previously established[10] for nine plumes from the Atlantic and Pacific, suggest that these plumes would become purely intraplate when the migrating ridge distance is $\sim 1{,}700 \pm 250$ km. At this point, both the topographic and the geochemical anomalies at the migrating ridge axis have disappeared (that is, subsided and contracted to zero). Additional arguments supporting this model of channelled plume dispersal are given elsewhere[10,22].

## Plume fluxes

Using the above tracer and topographic information, and the concept of buoyancy flux developed for intraplate plumes[7,13], I have developed two independent methods for constraining plumes fluxes, or plume discharge rates into migrating ridges.

Method 1 uses for constraint the length ($W$) of the geochemical anomaly and the nature of the geochemical gradient observed along the migrating ridge axis, for both the on-axis and the off-axis plume configurations shown in Fig. 2. Assuming symmetric conditions about the point of plume injection at $y = 0$,

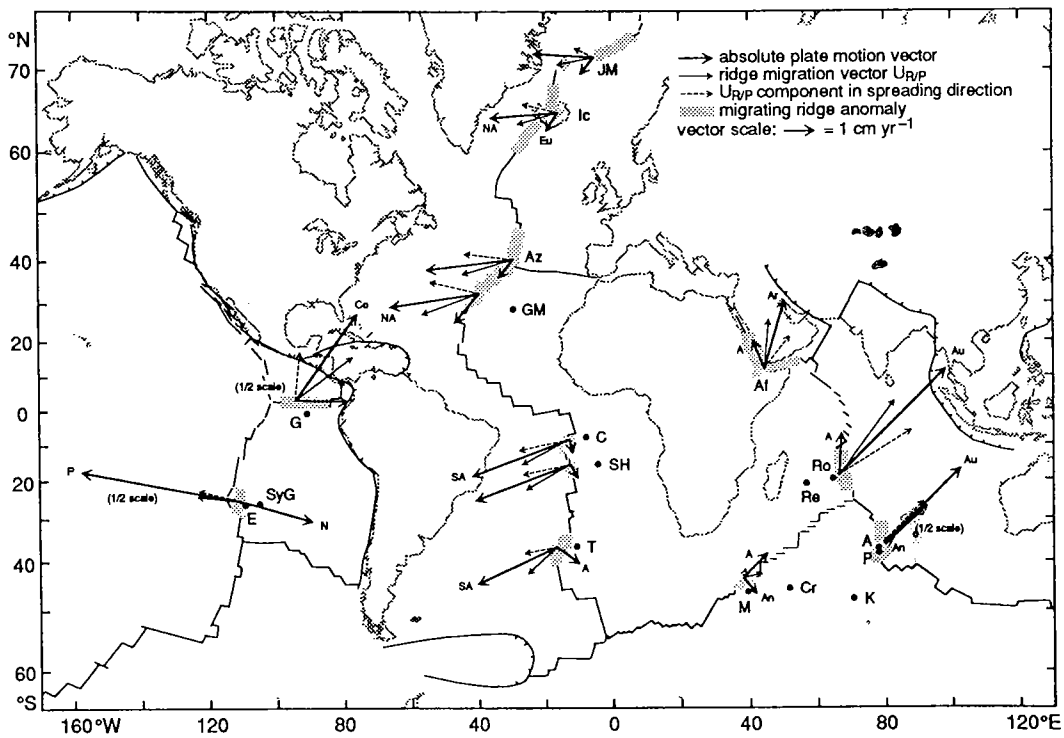


FIG. 1 Current plate motion and migrating ridge vector solutions of the 13 plume and migrating ridge systems investigated. The motion vectors are relative to the fixed hot-spot reference frame in model HS2 NUVEL-1 of Gripp and Gordon[60]. The abbreviated names of the hotspots are listed in Table 1. Related satellite islands discussed in ref. 22 are: A (Amsterdam); P (St Paul); M (Marion); Ro (Rodrigues); and E (Easter). Plate motion vectors are labelled as follows: A, Africa; An, Antarctic; Ar, Arabia; Au, Australia; Co, Cocos; Eu, Europe; Na, Nazca; NA, North America; P, Pacific; SA, South America.

and a steady state between the plume source and the ridge sink[10], the volumetric plume flux $Q_p$ is given by:

$$Q_p = 2k_1 \int_0^L H(y)S(y)P(y)\,dy = k_1 HSW/2 \qquad (1)$$

where $S(y)$ is the full spreading rate, $H(y)$ is the thickness of the fully developed lithosphere and $k_1$ is a coefficient described below. For a first-order integration, $S$ and $H$ were assumed constant and independent of $y$. Equation 1 also assumes for simplicity that the fraction, $P(y)$, of the plume contributing to the accretion process per unit ridge length, monitored by the isotopic gradient, decreases symmetrically and linearly with distance, $y$, along the ridge axis from the centre of the plume, that is $P(y) = 1-(y/L)$ (Fig. 2)[10].

For a ridge-centred plume (Fig. 2*a*), $Q_p$ is the total flux of the plume, whereas for the off-axis case (Fig. 2*b*) $Q_p$ represents only that portion of the plume that is channelled to the ridge axis. The coefficient $k_1$ then takes into account the fraction of the plume $[1-(1/k_1)]$ that does not enter the accretion process and may be dragged by the plates and dispersed into the asthenosphere on either side of the ridge axis in the direction $\pm x$ (Fig. 2). The inverse of $k_1 (0 \leq 1/k_1 \leq 1)$ is the fraction of the plume flux that is participating in the lithosphere accretion over the anomaly length $W$ (which is twice the integral in equation 1 divided by $Q_p$). Thus, $k_1$ must be greater than 1 and depends on the geometry of the kinematic model considered for the dispersal of the plume beneath the lithosphere.

Method 2 uses for constraints the excess elevation $\Delta E$, of the ridge axis associated with the geochemical anomaly (Fig 2), and the concept of the buoyancy flux[7,13], adapted to a ridge axis. For both the on-axis and off-axis plume configurations shown in Fig. 2, the mass production rate of excess ridge topography, $B$, assuming symmetry about the point source of plume injection at $y = 0$, is given by:

$$B = 2k_2(\rho_m - \rho_w)\int_0^L \Delta E(y)S(y)\,dy = k_2 \Delta E(o)SW(\rho_m - \rho_w)/2$$

The first-order integration was carried out by assuming that $S(y)$ is independent of $y$. It also assumes a linear gradient for the excess elevation of the ridge axis ($\Delta E$), symmetrically distributed about the centre of the plume (denoted o), that is $\Delta E(y) = \Delta E(o)(1-(y/L))$ (Fig. 2). The parameters $\rho_m$ and $\rho_w$ are the densities of the mantle (3,300 kg m$^{-3}$) and of water (1,000 kg m$^{-3}$). The coefficient $k_2 = (\Delta E(o) - \varepsilon)/\Delta E(o)$, with $0 \leq k_2 \leq 1$, corrects for the possible contribution of a thicker crust to the ridge elevation anomaly. The parameter $\varepsilon$ is the contribution to the elevation anomaly $\Delta E(o)$ observed over the point of plume injection, resulting from the thicker crust. It can be estimated from appropriate Airy compensation models, as discussed later.

If the buoyancy of the plume (per unit of gravitational acceleration) is purely of thermal origin, as assumed by Sleep[13], $B$ is also equal to:

$$B = k_2 \Delta E(o)SW(\rho_m - \rho_w)/2 = \Delta\rho_p Q_p = \rho_m \alpha \Delta T Q_p$$

where the parameter $\Delta\rho_p$ is the density reduction of the thermal plume relative to the ambient mantle, $\Delta T$ is the excess temperature of the plume relative to the asthenosphere and $\alpha$ is the thermal expansivity ($3 \times 10^{-5}$ K$^{-1}$). Solving for the volumetric plume flux $Q_p$ gives:

$$Q_p = [k_2 \Delta E(o)SW(\rho_m - \rho_w)]/[2\rho_m \alpha \Delta T] \qquad (2)$$

The volumetric flux of the 13 plumes investigated by these two methods are compared in Table 1 and Fig. 3*a*, assuming first $k_1 = k_2 = 1$, $H = 100$ km and $\Delta T = 225$ K. The choice of conditions facilitate comparison with Sleep's estimates of plume flux, monitored directly over the plume in off-axis or on-axis settings.

The validity of assuming that the excess temperature is constant will be examined in the next section.

The fluxes estimated by methods 1 and 2 correlate well for plumes at distances $x > 275$ km from the migrating ridges under scrutiny (Fig. 3*a*). Accordingly, we can infer that in these off-ridge cases, $k_1 = k_2 = 1$, and the plume discharge rates measured at these migrating ridges represent essentially the entire plume component reaching the migrating ridge. There is no detectable excess component of plume flow caused by plate drag, and the crust thickness is essentially normal. The length of the geochemical anomaly, $W$, reflects essentially the width of the lateral plume channel at its intersection with the ridge axis (Fig. 2*b*). The local variability of isotope ratios within the anomaly, which is usually greater in these off-axis plume settings[10,11], reflects incomplete mixing of entrained asthenospheric material

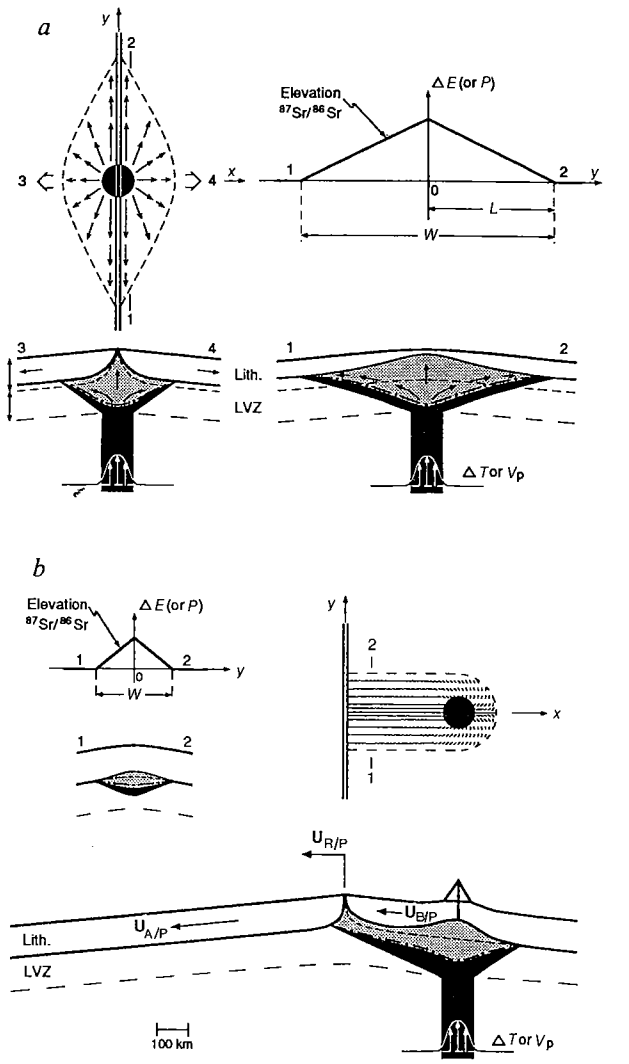


FIG. 2 Sketch of the MPS–MRS kinematic model in plan and section views, shown at two stages of evolution. *a*, Ridge-centred plume position; *b*, off-ridge plume position. Black regions represent the plume, shaded regions represent the zone of partial melting due to decompression. The dashed-dotted line is the solidus; the small dashed line is the base of normal lithosphere outside the thermally induced horizontal plume channel. The resulting excess elevation and strontium isotope gradients along the ridge axis are assumed to be linear in the model. Sections 1 and 2 are parallel, and sections 3 and 4 perpendicular to the ridge axis. $\boldsymbol{U}_{R/P}$, $\boldsymbol{U}_{A/P}$ and $\boldsymbol{U}_{B/P}$ are the horizontal velocity vectors of the migrating ridge axis (R), the plate (A) and the plate (B), relative to the vertical plume (P). $\boldsymbol{V}_p$ is the vertical velocity of the plume relative to the ambient mantle. The LVZ ('low-viscosity zone') is a layer of low seismic velocity underneath the lithosphere. See text for definition of other terms.

in the lateral channel (Fig. 2*b*). In contrast, in those settings where the plume is located close to or over the migrating ridge ($x < 275$ km), the coefficients $k_1$ and $k_2$ must be modelled.

The fraction of the plume flux $[1-(1/k_1)]$ that disperses into the low-viscosity zone (LVZ) without entering the accretion process can be estimated from the kinematic model proposed by Sleep[13] for the Iceland ridge-centred plume. Its flux is given by $Q_p = S(H+A/2)W$, where $A$ is the thickness of the LVZ. The model assumes that the component of the plume flow perpendicular to and symmetric about the ridge axis decreases linearly to zero with increasing depth across the LVZ because of plate drag (Fig. 2*a*). Combining this with equation 1 gives $k_1 = 2+(A/H)$. If $A = H$, as assumed by Sleep[13], $k_1 = 3$ in this particular case. I believe that this is likely to be an overestimate of $k_1$ for two reasons. First, Sleep's model apparently assumes that the accreting lithosphere over the geochemical anomaly length $W$ is composed entirely of plume material, whereas here I assume a linear geochemical gradient (see equation 1 and Fig. 2*a*) and thus that only half the lithosphere consists of plume material. Second, Sleep's model assumes that the component of the plume flux per unit ridge length perpendicular to the ridge axis, which is being dragged by the plates and dispersed into the LVZ, is constant along the entire length $W$. Again this is not compatible with the observed geochemical gradient, which suggests that the plume flow decreases outward along the ridge.

A more realistic kinematic plume model is to assume that the plume component per unit of ridge length that is dragged by the lithosphere on either side of the ridge axis decreases in the same linear proportion, $P(y) = 1-(y/L)$, as observed within the lithosphere, where the decrease is deduced from the geochemical tracers (Fig. 2*a*). It can easily be shown that this kinematic model corresponds to a plume flux $Q_p = S(H/2+A/4)W$. Assuming again that $A = H$ for ease of comparison with Sleep's plume fluxes, and combining with equation 1, we obtain $k_1 = 3/2$, which I believe is likely to be an upper limit for this coefficient.

The contribution $\varepsilon$ to the observed elevation anomaly $\Delta E(o)$, resulting from the presence of a thicker crust, can be estimated to first order from the Airy isostatic compensation models shown in Fig. 4. For the Azores submerged platform[23], underlain by an anomalously thick crust given by $H_c = 10$ km, and surrounded by a normal oceanic crust of thickness $h_c = 7$ km (Fig. 4*a*), $\varepsilon = H_c - h_c)\ (\rho_m - \rho_c)/(\rho_m - \rho_w)$, where $\rho_c$ is the density of the crust (2,900 kg m$^{-3}$). In this case $\varepsilon$ would be equal to 0.52 km, and accordingly $k_2 = 0.71$. The same value is assumed for the Jan Mayen platform because of the similar setting, as its crustal thickness is not yet documented.

In the case of the Iceland subaerial platform, the Airy model shown in Fig. 4*b* requires.

$$h_w = [(H_c - h_c)(\rho_m - \rho_c) - h_a\rho_m]/(\rho_m - \rho_w)$$

with, in this case, $\varepsilon = h_a + h_w$, where $h_a$ is the elevation above sea level over the plume, and $h_w$ is the water depth over the normal crust ($y > L$). The anomalous crustal thickness for Iceland is[24] $H_c = 16$ km, with a subaerial exposed part $h_a = 0.5$ km, $\varepsilon = 1.35$ km, and $k_2 = 0.6$. If $H_c$ for Iceland were 20 km, as assumed by McKenzie[25], then $k_2 = 0.4$, other things being equal. An average of $k_2 = 0.5$ is adopted for Iceland, for the Afar[26] and for Crozet[22], in view of their similarity in crustal thickness and structure[25]. The anomalous Galapagos spreading centre probably has a thicker crust than normal, requiring an Airy correction similar to the Azores ($k_2 = 0.7$), but it is sufficiently remote from the plume to assume $k_1 = 1$ ($x = 250$–$300$ km). Overall, it seems that without correcting for the possible presence of a thicker crust, the plume flux would be overestimated by 30–60% at most with method 2.

My 'best estimates' for the 13 plumes so far investigated (Table 1) are based on a simple average of the two methods with $k_1 = k_2 = 1$ for distant plumes ($x > 275$ km), and a weighted average, using the $k_1$ and $k_2$ values just discussed, for the ridge-centred plumes (Iceland, Afar and Crozet) and nearly ridge-centred plumes (Azores, Jan Mayen and the Galapagos). The volumetric flux of the 13 plumes investigated ranges from 0.4 km$^3$ yr$^{-1}$ for the Great Meteor to 3 km$^3$ yr$^{-1}$ for Kerguelen.

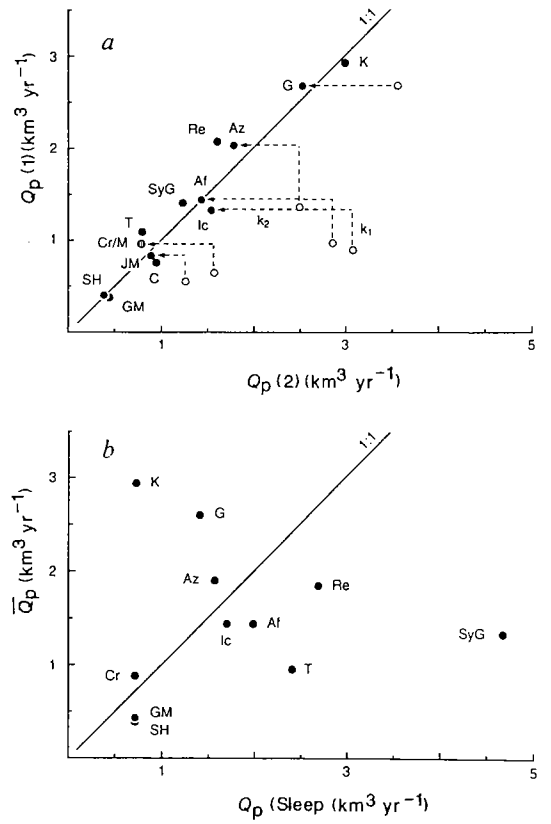


FIG. 3 Comparison of plume discharge rates at the migrating ridge axis $Q_p$, based on *a*, the isotope anomaly length (equation 1) and the excess ridge elevation anomaly (equation 2). Dashed lines show the effect of the coefficient $k_1$ (vertical) and $k_2$ (horizontal) for ridge-centred plumes ($x < 275$ *km*), as discussed in the text. *b*, Best estimate of the plume flux $\bar{Q}_p$ monitored at the migrating ridge axis (average of equations 1 and 2) against the plume flux of Sleep[13] estimated directly over the plume. The abbreviations for the plume names are given in Table 1.

TABLE 1 Volumetric flux and excess temperature of plumes

| Plume | Ridge anomaly | $W$ (km) | $\Delta E$(o)* (km) | Dist. ($x$) (km) | $S$ (mm yr$^{-1}$) | $Q_p$(1)† (km$^3$ yr$^{-1}$) | $k_1$ | $Q_p$(2)† (km$^3$ yr$^{-1}$) | $k_2$ | $\bar{Q}_p$‡ (km$^3$ yr$^{-1}$) | $Q_p$ (Sleep) (km$^3$ yr$^{-1}$) | $\Delta T$ ($K$) |
|---|---|---|---|---|---|---|---|---|---|---|---|---|
| North Atlantic | | | | | | | | | | | | |
| Jan Mayen (JM) | 71°–73° N | 668 | 2.2 | 75 | 16.6 | 0.55 | 1.5 | 1.26 | 0.71 | 0.86 | — | 242 |
| Iceland (I) | 60°–66° N | 923 | 3.4 | 0 | 19.0 | 0.88 | 1.5 | 3.08 | 0.50 | 1.43 | 1.98 | 263 |
| Azores (Az) | 33°–40° N | 1,094 | 1.8 | 100 | 24.6 | 1.35 | 1.5 | 2.50 | 0.71 | 1.90 | 1.56 | 198 |
| Great Meteor (GM) | 34°–36° N | 323 | 1.1 | 866 | 23.8 | 0.38 | 1 | 0.44 | 1 | 0.41 | 0.71 | 255 |
| South Atlantic | | | | | | | | | | | | |
| Circe (C) | 7°–11° S | 393 | 1.2 | 444 | 38.7 | 0.76 | 1 | 0.94 | 1 | 0.85 | — | 278 |
| St. Helena (SH) | 15°–16° S | 208 | 0.9 | 811 | 39.3 | 0.41 | 1 | 0.38 | 1 | 0.40 | 0.71 | 209 |
| Tristan (T) | 35°–40° S | 565 | 0.7 | 416 | 38.5 | 1.09 | 1 | 0.79 | 1 | 0.94 | 2.4 | 162 |
| Red Sea/Gulf of Aden | | | | | | | | | | | | |
| Afar (Af) | 42°–51° E | 1,000 | 2.9 | 0 | 19.1 | 0.96 | 1.5 | 2.86 | 0.50 | 1.44 | 1.7 | 224 |
| Pacific Ocean | | | | | | | | | | | | |
| Galapagos (G) | 95°–86° W | 880 | 1.3 | 255 | 60.2 | 2.65 | 1 | 3.56 | 0.71 | 2.60 | 1.4 | 214 |
| Sala y Gomez (SyG) | 25°–28° S | 350 | 0.85 | 730 | 80.0 | 1.40 | 1 | 1.23 | 1 | 1.31 | 4.67 | 197 |
| Indian Ocean | | | | | | | | | | | | |
| Crozet (Cr) | 43°–46° S | 788 | 2.38 | 1,128 | 16.2 | 0.64 | 1.5 | 1.57 | 0.50 | 0.87 | 0.71 | 184 |
| Kerguelen (K) | 33°–40° S | 862 | 1.0 | 1,412 | 67.2 | 2.90 | 1 | 2.99 | 1 | 2.94 | 0.71 | 232 |
| Reunion (Re) | 12°–22° S | 892 | 0.75 | 1,250 | 46.3 | 2.06 | 1 | 1.60 | 1 | 1.83 | 2.69 | 174 |

Sources of data for Indian Ocean and Sala y Gomez plumes are compiled in ref. 22; for other plumes see ref. 10.
* $\Delta E$(o) is the maximum excess elevation relative to 2.9 km normal mean depth[59].
† Given values of $Q_p$(1) and $Q_p$(2) are calculated using equations 1 and 2 with $k_1=1$ and $k_2=1$.
‡ Best estimate of plume flux $\bar{Q}_p=(k_1Q_p(1)+k_2Q_p(2)/2$ using the values of $Q_p$(1), $Q_p$(2), $k_1$ and $k_2$ given in the table.

For comparison, the plume flux at Hawaii, the largest currently active flux so far monitored[7,13], is 9–12 km$^3$ yr$^{-1}$. The estimate for Crozet (or Marion) is tentative at best as $W$ and $\Delta E$ are inadequately known[22].

The fraction of the plume flux radially dispersed into the LVZ (that is, not channelled towards the migrating ridge) can in principle be deduced from the difference between the plume flux estimated by Sleep[13] from the production of excess topography directly over the plume and the plume discharge rates estimated at the migrating ridge. Sleep's plume fluxes are plotted against the corresponding discharge rates estimated at the migrating ridge in Fig. 3*b*. The deviation from the mean of my flux and that of Sleep is generally ±20–60%, except for Sala y Gomez (Easter), Kerguelen and Tristan where it is ±90–120%. The difference are both positive and negative, and show no systematic trends with respect to the ridge migration distance $x$. Such trends might have been expected, as the lateral plume channel extends and cools with time, and some of the plume material may be dispersed and sink back into the underlying mantle. Some of the larger discrepancies between the two estimates of plume flux, monitored directly over the plume and at the intersection with the migrating ridge, are inherent in the choice of parameters used in the two models and can readily be reduced by normalization. For example, Sleep assumed a half-width ridge anomaly of 400 km comprising both Tristan and Gough hotspots, whereas I have used $L=250$ km for Gough only. For the Easter region, Sleep used a full spreading rate of 200 mm yr$^{-1}$ for the East Pacific Rise, whereas I used 80 mm yr$^{-1}$, as we have shown that only the east rift of the Easter microplate is affected by the Sala y Gomez plume[27–29]. As for the large negative discrepancy for Kerguelen, which is absurd, Sleep's flux estimate is not specific to this particular plume but generic to weak intraplate plumes at the detection limit of his method. In turn, it may be that my estimate made for the southwest Indian Ridge is related to the St Paul or Amsterdam plume instead of the more remote Kerguelen hotspot, as also evident from the isotope signals[22]. Overall, it thus seems likely that the discrepancies between Sleep's flux values and those obtained in my approach reflect the large errors involved in the calculations, which can easily reach 50% in my estimates. Nevertheless, the broad similarity of the plume fluxes estimated over the vertical plume and at the migrating ridge suggests that the discharge at the ridge can represent a substantial fraction of the total plume flux dispersed into the LVZ.

## Excess temperature of plumes

By equating the two plume flux methods 1 and 2 given above, I have solved for the mean excess temperature of plumes, which is given by:

$$\Delta T=[k_2(\rho_m-\rho_w)\Delta E(o)]/[k_1H\rho_m\alpha]$$
$$=232(k_2/k_1)\Delta E(o)$$

with $\Delta T$ in K and $\Delta E$(o) in km, $H=100$ km and the previously quoted values for $\rho_m$, $\rho_w$ and $\alpha$. Again, this assumes that the buoyancy of the plume is purely thermal in origin. The mean temperature excess of the plume is thus directly proportional to the maximum excess elevation on the ridge, within the uncertainty of the factor $(k_2/k_1)$. Without this correction, $\Delta T$ would be inversely related to the distance of the migrating ridge to the plume and range from 800 to 200 K (Fig. 5). We have just seen, however, that $(k_2/k_1)$ may range from 0.33 to 0.47 for ridge-centred plumes. With these corrections, and $k_1=k_2=1$ for the plumes more than 275 km from the ridge, the excess temperatures of the 13 plumes fall in the narrow range of 162 K (for Tristan) to 278 K (for Circe), including 263 K for Iceland, and their average is 215±35 K ($1\sigma$) (Table 1 and Fig. 5). The range quoted compares well with other estimates using independent methods and constraints. These vary from 100 K for Iceland[21] to 300 K for Hawaii[30], and are generally 200–250 K (refs. 7,13,25,31). The inversion performed by McNutt[32] indicates an excess temperature of 250–300 K at a depth of 50 km beneath Hawaii and the Marquesas. Finally, Sleep[13] has noted that the centre of these plumes may be 1.25 to 1.6 times as high as the mean excess temperature discussed here (estimated along the ridge axis over the length of the elevation and geochemical anomaly). Surprisingly, the excess temperature of the 13 plumes show no relation to the migrating ridge distance $x$, nor to their discharge rates at the migrating ridge. This observation has several implications.

First, it suggests that a quasi-steady thermal state is established rapidly at shallow depth, between the plume, the LVZ and the accreting and aging lithosphere, from the time these plumes were centred over the ridge to their present configurations

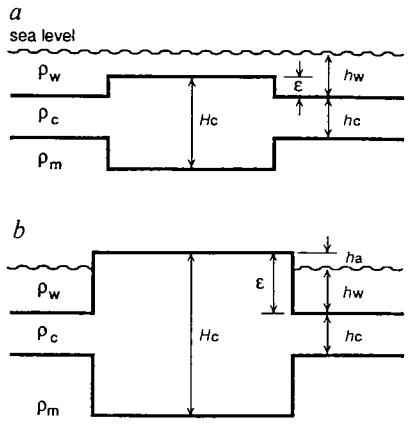


FIG. 4 Airy isostatic compensation models for ridge-centred plumes. *a*, Submerged platform (such as Azores); *b*, Subaerial platform (such as Iceland). See text for definition of terms.

(Fig. 1). Implicit in this MPS/MRS model is that the plume flow takes place mostly along a thermally induced groove and rounded channel carved by the hot plume at the base of the accreting lithosphere (Fig. 2). Using Turcotte and Oxburgh's thermal boundary-layer model[1] and a typical excess temperature of the plume of 200 K, I estimate[22] this thermal groove to be ~30 km deep, measured upward from the base of a fully developed lithosphere of 100 km thickness, and only 3 km deep near the migrating ridge axis where the lithosphere is only 10 km thick. The pressure gradient required to maintain this lateral plume flow toward the migrating ridge is provided by the dynamic pressure of the plume guided by the slope of the growing rigid lithosphere towards the ridge axis. Elsewhere[22], I present kinematic arguments that suggest that forces resulting from plate drag or large-scale return flows associated with the plate tectonic cycle have smaller effects. Assuming a Poiseuille type of conduit plume flow, 100 km in diameter and, 1,000 km long, with a 3 $km^3\ yr^{-1}$ flux and a viscosity of $3\times10^{18}$ Pa s, the mean pressure drop required would be 116 $Pa\ m^{-1}$, corresponding to a hydraulic head of 3.5 km. This is not impossible, as an inviscid plume from the core-mantle boundary[33], with a density contrast of 33 $kg\ m^{-3}$, would have a hydraulic head of 29 km.

Second, it is now established that the excess temperature of starting plume heads[34], as well as of plume conduits tilted by mantle winds[18,35], decreases as they rise and entrain the surrounding mantle. The magnitude of the entrainment depends on the buoyancy (heat) flux of the plume. Weak plumes (small flux) entrain and cool more than strong ones, other things being equal. Thus, for a given $\Delta T$ at the source, one would expect the $\Delta T$ of the conduit plumes in the upper mantle to be either inversely proportional to their depth of origin for equivalent fluxes, or directly proportional to their fluxes if they came from the same depth and had the same tilt. The latter conditions are evidently too restrictive, as the plume fluxes do not correlate with their excess temperatures in the upper mantle.

We also observe no apparent correlation between the excess temperature and the geochemical and isotopic composition of the plumes, as one might expect if some of the plumes under investigation came from the core-mantle boundary[36-38] and others from the 670-km discontinuity[39], or if some had been triggered at shallower depth by some kind of metasomatism[40]. For example, the high ratio $^3He/^4He$ in plumes such as Iceland is usually taken to indicate a derivation from the lower mantle[41], whereas low $^3He/^4He$ in plumes such as the Azores may reflect crustal recycling at shallower depths[42]. Yet the range of $\Delta T$ of plumes with high $^3He/^4He$ is 263 K (Iceland)[41] to 174 K (Reunion)[43], and for plumes with low $^3He/^4He$ it is 232 K (Kerguelen)[44] to 162 K (Tristan)[45]. The overlap is essentially complete.

A derivation from the lower mantle has also been suggested for plumes with the Dupal isotopic signature as a result of the coincidence of the Dupal anomaly with the second-harmonic residual geoid anomaly and P-wave velocity anomaly determined by seismic tomography[46-48]. But again there is no clear systematic relationship between $\Delta T$ and the isotopic characteristics. The $\Delta T$ of the Dupal plumes investigated from the South Atlantic and the Indian oceans is 162–232 K, whereas for the non-Dupal plumes $\Delta T = 170$–263 K. Again the overlap is complete. Thus, it also seems that the contents of the heat-generating elements uranium, thorium and potassium are not likely to be influential internal factors in controlling the excess temperature of these plumes. This has also been pointed out by Griffiths[49] on the basis of fluid-dynamic arguments.

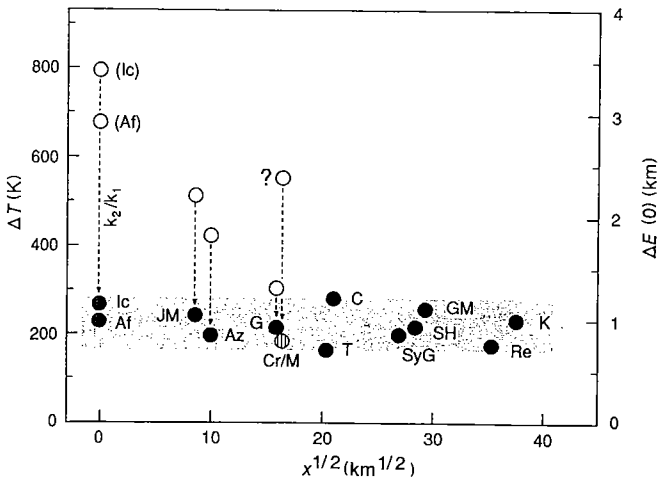


FIG. 5 Plume excess temperature plotted against the square-root of the distance to the migrating ridge. The square-root distance scale is used for visual convenience only. Vertical dashed lines show the effect of the coefficient $k_2/k_1$ for the ridge-centred plumes ($x < 275$ km) ○, uncorrected data for $x < 275$ km. Right axis shows corresponding maximum excess-elevation anomaly, $\Delta E(o)$, either observed (○, $x < 275$ km; ● for $x > 275$ km), or as given in Table 1 and discussed in the text. Note that the estimated excess temperatures of the plumes fall in the narrow range of 160–280 K (shaded region). The variation in $\Delta T$ is independent of the distance $x$ to the migrating ridge, the volumetric flux and the He, Pb, Nd and Sr isotope composition of these plumes. The abbreviations for the plume names are those given in Table 1.

At this stage and within the uncertainties in $\Delta T$s involved, which certainly are ±50 K, and could possibly reach 100 K, it would seem that a common depth of origin and regulated source of heat is indicated by the relative constancy of the estimated excess temperatures of the 13 plumes investigated. The D″ thermal boundary layer at the core-mantle interface is the most likely place[36–38]. If so, then what caused the large diversity in isotope and trace element ratios among these plumes? Perhaps the geochemical and isotopic diversity of plumes, and their temporal variation so far documented, reflect the layered nature and timing of the recycled lithosphere material accumulating and forming the D″ layer, the mode of subsequent plume detachments and the complexities of the entrainment process, particularly across the 670-km discontinuity where some recycled material may also have accumulated[39,50,51].

It is of interest to note that Bonatti[52] has described the mantle underlying the Azores as "not so hot" on the basis of geothermometry of peridotites from the region. The Azores is a low $^3He/^4He$ 'wet' plume highly enriched in volatiles[40]. My estimate of its excess temperature, however, is 198 K, well within the range of other plumes. Therefore, this claim cannot be confirmed, unless it could be demonstrated that in this case the buoyancy flux of the plume is of chemical rather than of thermal origin, but this is doubtful.

Estimates of plume excess temperatures by my method could be improved in the future with new information on crustal thicknesses associated with these anomalous migrating ridge segments, with improved topographic maps and sampling, and by adding constraints from geoid data. Distinguishing between plume origins from estimates of excess plume temperatures is likely to be a difficult task, however, because of the uncertainties involved in the method and in the effect of entrainment on the excess temperature in the plume conduit as a function of depth, which remain poorly constrained and quantified.

## Other dynamic effects

Finally, there is ample evidence that plumes feeding migrating ridges can have other important dynamic and tectonic effects, apart from topographic uplift. They can generate the propagation of rifts[53] and development of transient microplates[27], and induce rift jumps back towards the plume, and as a result, large transform-fault offsets[54]. Variations in isotope tracer concentrations across these transform-fault discontinuities testify that conduit plumes do not disperse radially into the LVZ, but are preferentially channelled as the MPS/MRS model predicts[10,53]. Apparently, the only time that plumes may disperse radially into the upper mantle may be when an initial plume head reaches and flattens against a rather stationary plate, such as a subcontinental lithosphere. Evidence for a vestige of the dispersal of St Helena and Tristan plume heads under the Gondwana continental lithosphere has been detected[12] along the Mid-Atlantic Ridge between 20° S and 40° S. Also, variations in the isotope tracers neodymium, strontium and lead along the Gulf of Aden and Red Sea suggest that the head of the Afar plume may have recently been flattened and radially dispersed[55].

The bending of plumes into the LVZ towards migrating ridges, and their temperature structure, also have important effects on the outgassing of plumes and the local decoupling of the $^3He/^4He$ ratio from the isotope tracers, as well as the petrology of melting products directly over the plume, along the channel and at the migrating ridge axis. These topics are considered elsewhere[22], in conjunction with the study of the tilting of some of these plumes by mantle winds[18,56], as a possible alternative to the MPS/MRS model discussed here. But that study indicated that tilting by mantle winds was insufficient to explain the observations and the MPS/MRS model is still preferred as the dominant mechanism affecting the topography and geochemistry of mid-ocean ridges migrating away from plumes.

Geophysicists have yet to find a ridge that is currently migrating towards a fixed plume, and that has an isotope signature clearly distinguishable from the depleted asthenosphere usually feeding mid-ocean ridges; such a situation would allow the dynamics of plume–ridge interaction to be studied further. This was thought to be the case for the Juan de Fuca Ridge with respect to the Heck–Heckle–Springfield seamount chain[57], but lava from these seamounts has mainly been found to be normal MORB-like and different from those found on the nearby Endeavor ridge segment[58]. The search continues. □

Received 2 May; accepted 27 June 1991.


1. Turcotte, D. L. & Oxburgh, E. R. *J. Fluid Mech.* **28,** 29–42 (1967).
2. Olson, P., Silver, P. G. & Carlson, R. W. *Nature* **344,** 209–215 (1990).
3. Bercovici, D., Schubert, G. & Glatzmaier, G. A. *Science* **244,** 950–955 (1989).
4. Davies, G. F. *J. geophys. Res.* **89,** 6017–6040 (1984).
5. Stein, S., Melosh, H. J. & Minster, J. B. *Earth planet. Sci. Lett.* **36,** 51–62 (1977).
6. Richards, M. A., Hager, B. H. & Sleep, N. H. *J. geophys. Res.* **93,** 7690–7708 (1988).
7. Davies, G. F. *J. geophys. Res.* **93,** 10467–10480 (1988).
8. Cazenave, A., Souriau, A. & Dominh, K. *Nature* **340,** 54–57 (1989).
9. Dziewonski, A. M. & Anderson, D. L. *Am. Scient.* **72,** 483–494 (1984).
10. Schilling, J.-G. *Nature* **314,** 62–67 (1985).
11. Schilling, J.-G., Thompson, G., Kingsley, R. & Humphris, S. *Nature* **313,** 187–191 (1985).
12. Hanan, B. B., Kingsley, R. H. & Schilling, J.-G. *Nature* **322,** 137–144 (1986).
13. Sleep, N. H. *J. geophys. Res.* **95,** 6715–6736 (1990).
14. White, R. & McKenzie, D. *J. geophys. Res.* **94,** 7685–7729 (1989).
15. Allègre, C. J., Hamelin, B. & Dupré, B. *Earth planet. Sci. Lett.* **71,** 71–84 (1984).
16. Skilbeck, J. N. & Whitehead, J. A. Jr *Nature* **272,** 499–501 (1978).
17. Olson, P. & Singer, H. *J. Fluid. Mech.* **158,** 511–531 (1985).
18. Richards, M. A. & Griffiths, R. W. *Nature* **342,** 900–902 (1989).
19. Morgan, W. J. *J. geophys. Res.* **83,** 5355–5360, (1978).
20. Vogt, P. R. *Earth planet. Sci. Lett.* **13,** 153–160 (1971).
21. Schilling, J.-G. *Nature* **242,** 565–571 (1973).
22. Schilling, J.-G. *J. geophys. Res.* (submitted).
23. Searle, R. *Earth planet. Sci. Lett.* **51,** 415–434 (1980).
24. Palmason, G. *Visindafelag Iseldinga* **XL,** 187 (Reykjavik, 1971).
25. McKenzie, D. *J. Petrol.* **25,** 713–765 (1984).
26. Schilling, J.-G. *Nature phys. Sci.* **242,** 2–5 (1973).
27. Schilling, J.-G., Sigurdsson, H., Davies, A. N. & Hey, R. N. *Nature* **317,** 325–331 (1985).
28. Hanan, B. B. & Schilling, J.-G. *J. geophys. Res.* **94,** 7432–7448 (1989).
29. Fontignie, D. & Schilling, J.-G. *Chem. Geol.* **89,** 209–241 (1991).
30. Wyllie, P. J. *J. geophys. Res.* **93,** 4171–4181 (1988).
31. Klein, E. M. & Langmuir, C. H. *J. geophys. Res.* **92,** 8089–8115 (1987).
32. McNutt, M. in *Seamounts, Islands and Atolls* (eds Keating, B. H., Fryer, P., Batiza, R. & Boehlert, G. W.) 123–132 (American Geophysical Union, Washington DC, 1987).
33. Sleep, N. H., Richards, M. A. & Hager, B. H. *J. geophys. Res.* **93,** 7672–7689 (1988).
34. Griffiths, R. W. & Campbell, I. H. *Earth planet. Sci. Lett.* **99,** 66–78 (1990).
35. Griffiths, R. W. & Campbell, I. H. *Earth planet. Sci. Lett.* **103,** 214–227 (1991).
36. Morgan, W. J. *Nature* **230,** 42–43 (1971).
37. Hofmann, A. W. & White, W. M. *Earth planet. Sci. Lett.* **57,** 421–436 (1982).
38. Olson, P., Schubert, G. & Anderson, C. *Nature* **327,** 409–413 (1987).
39. Allègre, C. J. & Turcotte, D. L. *Geophys. Res. Lett.* **12,** 207–210 (1985).
40. Schilling, J.-G., Bergeron, M. B. & Evans, R. *Phil. Trans. R. Soc.* A**297,** 147–178 (1980).
41. Poreda, R., Schilling, J.-G. & Craig, H. *Earth planet. Sci. Lett.* **78,** 1–17 (1986).
42. Kurz, M. D., Jenkins, W. J., Schilling, J.-G. & Hart, S. R. *Earth planet. Sci. Lett.* **58,** 1–14 (1982).
43. Graham, D., Lupton, J., Albaréde, F. & Condomines, M. *Nature* **347,** 545–548 (1990).
44. Vance, D., Stone, J. O. H. & O'Nions, R. K. *Earth planet. Sci. Lett.* **96,** 147–160 (1989).
45. Kurz, M. D., Jenkins, W. J. & Hart, S. R. *Nature* **297,** 43–47 (1982).
46. Dupré, B. & Allègre, C. J. *Nature* **303,** 142–146 (1983).
47. Hart, S. R. *Nature* **309,** 753–757 (1984).
48. Castillo, P. *Nature* **336,** 667–670 (1988).
49. Griffiths, R. W. *Earth planet. Sci. Lett.* **78,** 435–446 (1986).
50. Ringwood, A. E. & Irifune, T. *Nature* **331,** 131–136 (1988).
51. Kincaid, C. & Olson, P. *J. geophys. Res.* **92,** 13832–13840 (1987).
52. Bonatti, E. *Science* **250,** 107–111 (1990).
53. Schilling, J.-G., Kingsley, R. & Devine, J. D. *J. geophys. Res.* **87,** 5593–5610 (1982).
54. Burke, K., Kidd, W. S. F. & Wilson, J. T. *Nature* **241,** 128–129 (1973).
55. Schilling, J.-G., Kingsley, R. H., Hanan, B. B. & McCully, B. L. *J. geophys. Res.* (submitted).
56. Richards, M. A. & Griffiths, R. W. *Geophys. J.* **94,** 367–376 (1988).
57. Davis, E. E. & Karsten, J. L. *Earth planet. Sci. Lett.* **79,** 385–396 (1986).
58. Karsten, J. L., Delaney, J. R., Rhodes, J. M. & Liias, R. A. *J. geophys. Res.* **95,** 19235–19256 (1990).
59. Vogt, P. R., *Earth planet. Sci. Lett.* **29,** 309–325 (1976).
60. Gripp, A. E. & Gordon, R. G. *Geophys. Res. Lett.* **17,** 1109–1112 (1990).


ACKNOWLEDGEMENTS. I thank R. Kingsley and B. McCully for their assistance in gathering data, and K. Carey for editing. I also thank L. Fleitout for a discussion on the Airy isostatic compensation model. This work was supported by the NSF.